The Plant Cell, Vol. 8, 985–999, June 1996 © 1996 American Society of Plant Physiologists

MPG1 Encodes a Fungal Hydrophobin Involved in Surface Interactions during Infection-Related Development of *Magnaporthe grisea*

Nicholas J. Talbot,[a,1] Michael J. Kershaw,[a] Gavin E. Wakley,[a] Onno M. H. de Vries,[b] Joseph G. H. Wessels,[b] and John E. Hamer[c]

[a] Department of Biological Sciences, University of Exeter, Washington Singer Laboratories, Perry Road, Exeter EX4 4QG, United Kingdom

[b] Department of Plant Biology, University of Groningen, Kerklaan 30, 9751 NN Haren, The Netherlands

[c] Department of Biological Sciences, Hansen Life Science Research Building, Purdue University, West Lafayette, Indiana 47907-1392

The rice blast fungus expresses a pathogenicity gene, *MPG1*, during appressorium formation, disease symptom development, and conidiation. The *MPG1* gene sequence predicts a small protein belonging to a family of fungal proteins designated hydrophobins. Using random ascospore analysis and genetic complementation, we showed that *MPG1* is necessary for infection-related development of *Magnaporthe grisea* on rice leaves and for full pathogenicity toward susceptible rice cultivars. The protein product of *MPG1* appears to interact with hydrophobic surfaces, where it may act as a developmental sensor for appressorium formation. Ultrastructural studies revealed that *MPG1* directs formation of a rodlet layer on conidia composed of interwoven ~5-nm rodlets, which contributes to their surface hydrophobicity. Using combined genetic and biochemical approaches, we identified a 15-kD secreted protein with characteristics that establish it as a class I hydrophobin. The protein is able to form detergent-insoluble high molecular mass complexes, is soluble in trifluoroacetic acid, and exhibits mobility shifts after treatment with performic acid. The production of this protein is directed by *MPG1*.

INTRODUCTION

Many pathogenic fungi infect plants by elaborating specialized cells known as appressoria. These cells are spherical or dome shaped and differentiate from the ends of fungal germ tubes. Production of appressoria is unique to parasitic fungi and depends greatly on the ability of fungal hyphae to attach to and perceive an appropriate surface. Appressorial morphogenesis has been studied in a variety of fungal pathogens by use of cytological methods (Mendgen and Deising, 1993), but little is known about the underlying molecular biology. In view of the overriding importance of surface interactions to fungi, dissecting the mechanisms of surface perception, attachment, and transduction of extracellular physical stimuli may be central to understanding fungal infection–related development. The rice blast fungus *Magnaporthe grisea* is an experimentally tractable fungus, and this has allowed the characterization of a number of processes central to appressorium development (reviewed in Talbot, 1995).

Recently, we identified a gene from *M. grisea* that is highly expressed during pathogenesis and plays an important role in appressorium development (Talbot et al., 1993a). This gene, named *MPG1*, was identified based on its preferential expression during fungal growth in plant tissue, being most abundantly expressed during the prepenetration phase of development and during expression of disease symptoms. Critically, *mpg1*$^-$ mutants generated by a one-step gene replacement are less pathogenic than the wild type and produce a smaller number of lesions (Talbot et al., 1993a). This infection deficiency phenotype was attributed to a reduced ability of the fungus to form appressoria (Talbot et al., 1993a).

The sequence of the *MPG1* gene predicted a protein homologous with the fungal hydrophobins (Talbot et al., 1993a). These proteins are small, secreted, hydrophobic polypeptides characterized by the conserved spacing of eight cysteine residues (Wessels, 1994). Hydrophobins have been found in aerial and developmental structures of fungi (Stringer et al., 1991; Wessels et al., 1991a; Bell-Pederson et al., 1992; Lauter et al., 1992). Two hydrophobin-like proteins are also implicated as fulfilling a role as phytotoxins, although this role has yet to be confirmed (Zhang et al., 1992; Bowden et al., 1994).

Sc3p from the basidiomycete *Schizophyllum commune* is the only hydrophobin to have been purified and studied in detail. This work led to the remarkable discovery that the protein self-assembles into an amphipathic "membrane" structure when it encounters a gas–water interface or a hydrophobic

[1] To whom correspondence should be addressed.

surface (Wösten et al., 1993, 1994b). When examined by electron microscopy, the assembled protein complex has a rodlet structure on its hydrophobic side (Wösten et al., 1993) that is identical to the rodlet layer found on the surface of aerial hyphae of the fungus (Wösten et al., 1994a).

The overall amino acid identity among hydrophobins is low (11%), suggesting that they possess diverse properties (Wessels, 1992, 1994). For example, two hydrophobin "toxins," cryparin and cerato-ulmin (Zhang et al., 1992; Bowden et al., 1994), show hydropathy profiles and biochemical properties distinct from those of other known hydrophobins (see results below). In light of these differences, they have recently been named class II hydrophobins (Wessels, 1994) to distinguish them from the class I hydrophobin genes found in *S. commune, Neurospora crassa, Aspergillus nidulans, Metarhizium anisopliae,* and *M. grisea* (Schuren and Wessels, 1990; Stringer et al., 1991; Lauter et al., 1992; St. Leger et al., 1992; Talbot et al., 1993a; Stringer and Timberlake, 1995). Mutant phenotypes for the hydrophobin-encoding genes have confirmed their role as spore wall proteins in *A. nidulans* (Stringer et al., 1991; Stringer and Timberlake, 1995) and *N. crassa* (Beever and Dempsey, 1978; Bell-Pederson et al., 1992; Lauter et al., 1992), whereas *Sc3*$^-$ mutants display reduced aerial hyphae formation and surface adhesion (Wösten et al., 1994b). Targeted mutation of *MPG1* also caused not only a reduction in cell surface hydrophobicity (Talbot et al., 1993a) but also a drastic reduction in the ability of *M. grisea* to form two distinct developmental stages in its life cycle: appressoria and conidia.

To address the role of *MPG1* in appressorium development, we sought to identify the potential protein product of *MPG1* and to study its physical and biochemical characteristics. We provide genetic evidence that *MPG1* is required for appressorium development and pathogenicity and is sufficient to restore these abilities. We show that *MPG1* directs both the formation of a rodlet layer on conidia and the production of a protein with characteristics of a class I hydrophobin. Attachment assays suggest a role for this protein in the interaction of germ tubes and appressoria with hydrophobic surfaces during infection-related development.

RESULTS

Genetic Analysis of *mpg1*::*Hph* Strains of *M. grisea*

Hygromycin-resistant *mpg1*$^-$ mutant strains generated by gene replacement (*mpg1*::*Hph*) show a number of concurrent phenotypes, including reduced pathogenicity, reduced appressorial development, reduced conidiation, and an "easily wettable" phenotype (Talbot et al., 1993a). To ensure that these phenotypes are all caused by the gene disruption event, a genetic cross was performed between the *mpg1*::*Hph* transformant TM400-2 and a wild-type nonisogenic rice pathogen of the opposite mating type, TH3. Sixty-three random ascospore progeny were selected, and hygromycin resistance was found to segregate in the ratio of 29 resistant:34 susceptible, suggesting segregation of a single gene (χ^2 = 0.40; $P > 0.1$). A representative sample of 20 progeny was then taken, and DNA gel blot analysis was conducted to determine the segregation of the *Hph* (hygromycin phosphotransferase–encoding) and *MPG1* genes, as shown in Figure 1A. The blots revealed complete cosegregation of *Hph* with the *mpg1*$^-$ null mutation; this finding confirmed that there was a single site of integration of the gene replacement vector at the *MPG1* locus.

Pathogenicity assays were performed, and leaves taken from plants inoculated with four representative progeny are shown in Figure 1B. Progeny 53-R-8 and 53-R-21, which carry the *MPG1* gene (leaves A and C), caused large spreading lesions on leaves of the susceptible rice cultivar CO-39, as did the wild-type strain Guy-11 (leaf E). However, the *mpg1*$^-$ mutant progeny 53-R-10 and 53-R-39 (leaves B and D) showed far fewer lesions, as did the *mpg1*::*Hph* parent TM400-2 (leaf F). The mean lesion density measured for 5-cm-long leaf tips was 3.4 among *mpg1*$^-$ progeny, as compared with 12.04 for wild-type progeny (Student's *t* test, t = 11.97; $P < 0.001$; degrees of freedom = 980). The *mpg1*$^-$ segregants 53-R-10 and 53-R-39 also produced significantly fewer appressoria when compared with wild-type progeny 53-R-8 and 53-R-21. This finding was based on direct observations of rice leaves, as shown in Figures 2A to 2E, or by assays performed on Teflon membranes. The mean frequency of appressorium formation among all of the *mpg1*$^-$ mutant 53-R progeny was 20.25% (SD = 8.12), as compared with 78.55% (SD = 11.64) for wild-type progeny (χ^2 = 43.27; $P < 0.001$). The Mpg1 phenotype was striking when mutants were observed on rice leaves. Very long germ tubes that ended by hooking around the waxy projections on the leaf surface were often observed (Figures 2B and 2F).

Variability in the production of conidia and the formation of appressoria was observed in 53-R progeny, as shown in Table 1, although a significant difference between wild-type and *mpg1*::*Hph* segregants was always apparent. The variability is probably due to the fact that the parental strains from the cross were nonisogenic, suggesting that severity of the mutant phenotype might be affected by allelic differences at a number of other loci.

Cosegregation of the easily wettable phenotype with the *mpg1*$^-$ mutation was also observed. Sporulating cultures from *mpg1*$^-$ progeny were easily wetted with water when compared with wild-type cultures; this observation suggests a difference in cell surface hydrophobicity (data not shown). From these observations, we conclude that all of the phenotypes observed in the gene replacement mutants are associated with the *mpg1*$^-$ mutation.

Reintroduction of *MPG1* Restores Pathogenicity

To determine whether *MPG1* is sufficient to complement all of the observed Mpg1 mutant phenotypes, a 3.75-kb genomic fragment containing the *MPG1* gene was transformed into 53-R-39. This fragment has been completely sequenced (Talbot

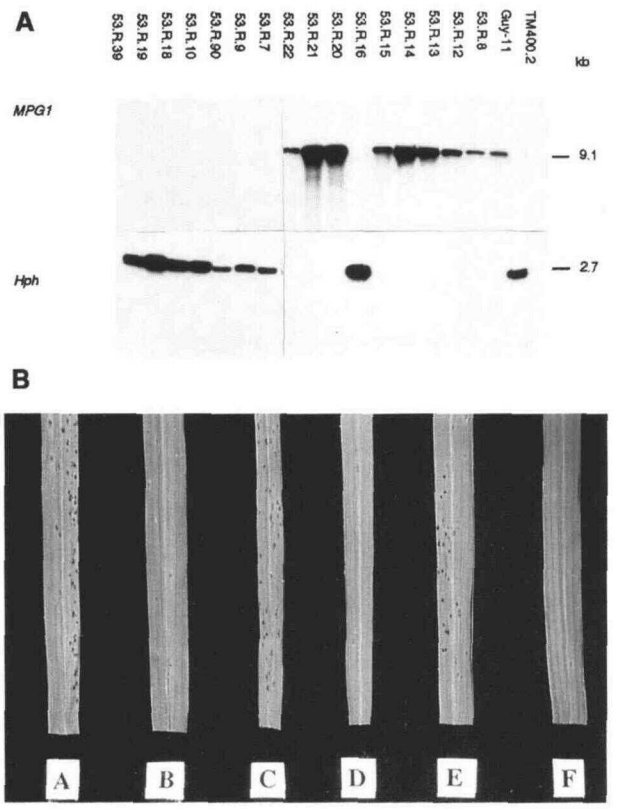

Figure 1. Random Ascospore Analysis of the *mpg1*::*Hph* Gene Replacement and Segregation of Pathogenicity.

(A) DNA gel blot hybridizations were performed to determine segregation of the *mpg1*::*Hph* deletion allele in random ascospore progeny. The progeny were generated from a cross between the *mpg1*::*Hph* transformant TM400-2 (*Mat1-2*) and the wild-type strain TH3 (*Mat1-1*). Progeny 53-R-7, 53-R-9, 53-R-10, 53-R-16, 53-R-18, 53-R-19, 53-R-39, and 53-R-90 are hygromycin B–resistant segregants; all others shown are hygromycin B sensitive. In the top panel, DNA was digested with EcoRI, fractionated in a 0.8% agarose gel, blotted to Hybond N, and hybridized with an *MPG1* cDNA insert from pNJT-15. *MPG1* hybridizes with a 9.1-kb EcoRI fragment in wild-type strains. Below, DNA from the same progeny was digested with XbaI, fractionated in a 0.8% agarose gel, blotted to Hybond N, and hybridized with a 2.7-kb XbaI fragment from pNT25 containing the *Hph* gene cassette (Talbot et al., 1993a).

(B) Conidial suspensions were prepared from random ascospore progeny and sprayed onto 14-day-old seedlings of the compatible rice cultivar CO-39. The plants were incubated to allow disease development for 96 hr. Shown are leaves from plants inoculated with the following strains: leaf A, hygromycin B–sensitive strain 53-R-8; leaf B, hygromycin B–resistant strain 53-R-10; leaf C, hygromycin B–sensitive strain 53-R-21; leaf D, hygromycin B–resistant strain 53-R-39; leaf E, wild-type strain Guy-11; and leaf F, *mpg1*::*Hph* strain TM400-2.

et al., 1993a) and contains a single open reading frame. Bleomycin-resistant transformants containing this insert were selected, and DNA gel blot analysis was performed to confirm introduction of *MPG1* and the bleomycin resistance gene, as shown in Figure 3A. Two independent transformants, MJK16 and MJK13, were tested for pathogenicity, appressorium development on rice leaves, conidial production, and wettability. All of the mutant phenotypes were fully complemented by introduction of *MPG1* (Figures 3B, 3D, and 3F).

MPG1 Produces a Conidial Wall Layer Composed of 5-nm-Diameter Rodlets

Expression of *MPG1* during conidiation and its relatedness to hydrophobin-encoding genes suggested that it might encode a component of conidial walls. To test this hypothesis, we conducted freeze–fracture experiments and examined carbon–platinum replicas of conidial walls by transmission electron microscopy. These studies revealed the presence of a wall layer composed of interwoven rodlets with an apparent diameter of 5 nm (±2 nm) on conidia of wild-type *M. grisea* strains, as shown in Figure 4B. This finding compares with the much larger and more typical 10- to 12-nm rodlets observed on conidial surfaces of *A. nidulans* (Figure 4A). The rodlet layer was completely absent from conidia of the *mpg1*::*Hph* transformant TM400-2 (Figure 4C), which possessed a smooth surface stippled with small, irregular ~10-nm-diameter projections. Analysis of 20 of the 53-R progeny showed that the presence of the rodlet layer completely cosegregated with the *MPG1* gene. Electron micrographs of the surface topology of conidia from two representative segregant progeny are shown in Figures 4D and 4E. Freeze–fracture experiments showed that this rodlet protein is associated with conidia but not with aerial hyphae (data not shown). This finding was confirmed by the fact that the easily wettable phenotype of *mpg1*::*Hph* strains was observed only in conidiating cultures and not in those with aerial hyphae only (data not shown).

To determine whether *MPG1* is sufficient to restore rodlet formation, freeze–fracture experiments were performed on conidia from the bleomycin-resistant *MPG1* transformants MJK13 and MJK16 containing the reintroduced *MPG1* gene. The recipient strain 53-R-39 had no rodlet layer (Figure 4F), whereas both transformants possessed an intact rodlet layer indistinguishable from wild-type strains. The rodlet layer from MJK16 is shown in Figure 4G.

MPG1 Directs Formation of a Class I Hydrophobin

The only class I hydrophobin to be completely purified is the product of the *Sc3* gene from *S. commune*. This hydrophobin was purified on the basis of its ability to aggregate at an air–water interface converting the protein monomers into high molecular weight SDS-insoluble aggregates (Wösten et al., 1993, 1994a). The protein was also found as an aggregate in hyphal

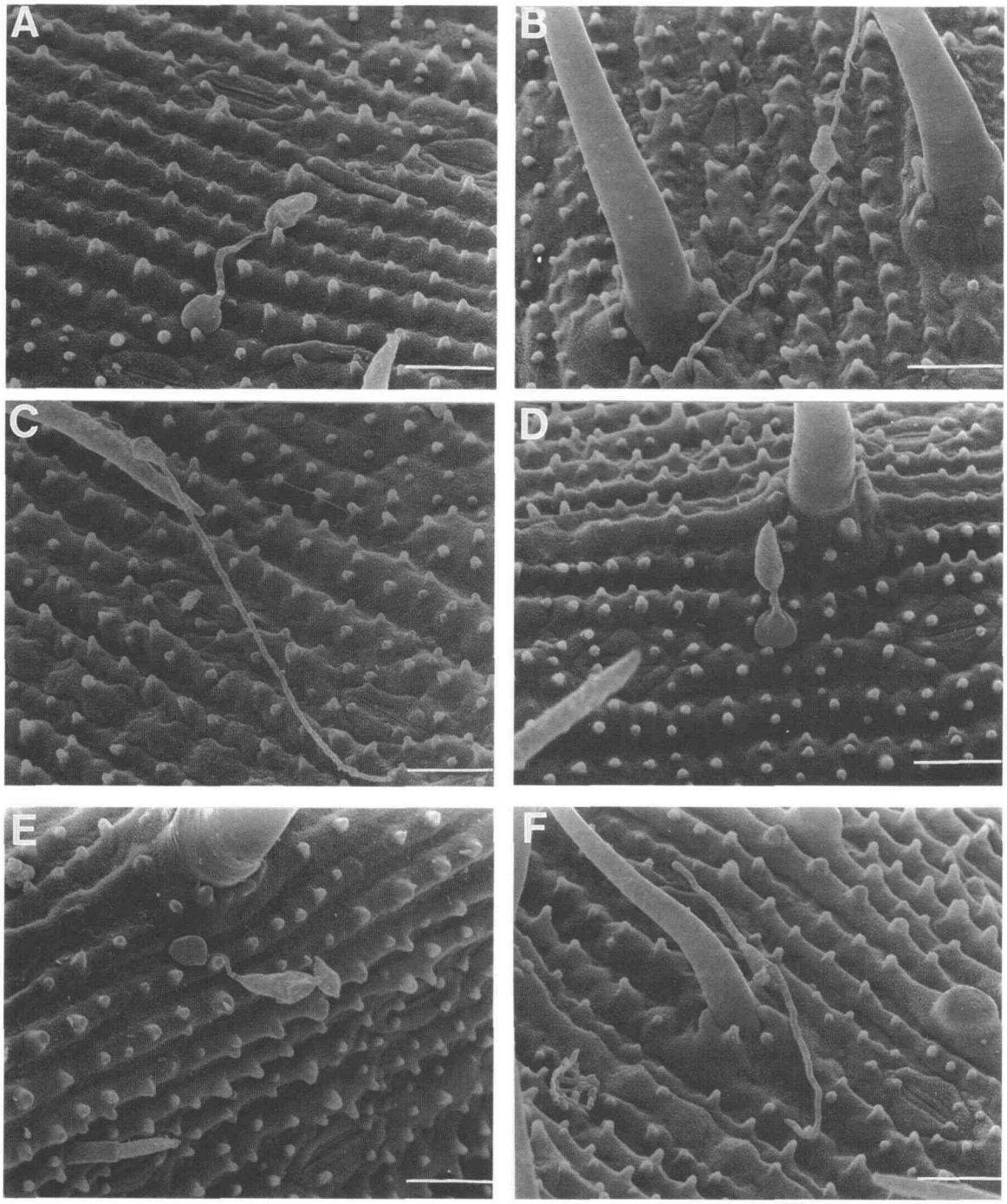

Figure 2. Cosegregation of the Appressorium Deficiency Phenotype with the *mpg1::Hph* Deletion Allele.

Conidial suspensions were prepared from random ascospore progeny and tested for their ability to elaborate appressoria on rice leaves. Scanning electron microscopy was used to photograph the surface of rice leaves. Appressoria are the hemispherical structures differentiating from the ends of germ tubes after conidial germination. *Mpg1* mutants produced predominantly long, undifferentiated germ tubes on rice leaves.

(A) Guy-11.

(B) *mpg1::Hph* transformant TM400-2.

(C) Hygromycin B–resistant segregant 53-R-10.

(D) Hygromycin B–sensitive segregant 53-R-8.

(E) Hygromycin B–sensitive segregant 53-R-21.

(F) Hygromycin B–resistant segregant 53-R-39.

Bars = 20 μm.

Table 1. Segregation Analysis of Mpg1 Mutant Phenotypes

Strain	Hygromycin Resistance[a]	Easily Wettable Phenotype[b]	Conidia Formation (mL^{-1})[c]	Appressorium Formation (%)[d]
Guy-11	S	+	3.3×10^6	78.0
TM400-2	R	Eas	3.7×10^5	18.3
TM400-5	R	Eas	1.0×10^5	20.6
53-R-7	R	Eas	6.3×10^5	23.6
53-R-9	R	Eas	1.3×10^5	9.6
53-R-10	R	Eas	2.2×10^5	31.0
53-R-16	R	Eas	3.6×10^5	20.6
53-R-18	R	Eas	5.1×10^5	23.3
53-R-19	R	Eas	7.7×10^5	28.8
53-R-39	R	Eas	3.9×10^5	9.4
53-R-90	R	Eas	1.9×10^5	15.7
53-R-8	S	+	2.1×10^6	87.8
53-R-12	S	+	2.2×10^6	70.6
53-R-13	S	+	5.6×10^6	94.8
53-R-14	S	+	2.3×10^6	81.3
53-R-15	S	+	2.1×10^6	63.7
53-R-20	S	+	1.4×10^6	92.8
53-R-21	S	+	1.1×10^6	82.6
53-R-22	S	+	5.1×10^6	80.5
53-R-35	S	+	2.0×10^6	62.1
53-R-40	S	+	2.3×10^6	69.3

[a] Resistance to 10^0 μg mL^{-1} hygromycin B. S, sensitive; R, resistant.
[b] Easily wettable phenotype was tested by placing a 10-μL water drop on the surface of aerial hyphae for 12 hr. Eas, a water-soaked appearance; (+), drop of water remained on the fungus surface.
[c] Conidia formation was tested by flooding a plate with 3 mL of water and counting conidia per milliliter. Value given is the mean from three experiments (range for wild-type conidiation, 2.8 to 8.0 $\times$ 10^6 mL^{-1} on complete media).
[d] Appressorium formation was tested on Teflon membranes. Values given are the mean number of conidia elaborating an appressorium after 12 hr in two independent experiments. The range for wild-type appressorium formation is typically 58 to 98%; the range for *Mpg1* mutants is typically 7 to 25%.

walls from aerial structures but interestingly not from submerged hyphae (Wessels et al., 1991a). The SDS-insoluble aggregates could be solubilized in either ice-cold formic acid or trifluoroacetic acid (TFA) (de Vries et al., 1993). Conversely, cerato-ulmin and cryparin, class II hydrophobins (Wessels, 1994), show different physical characteristics and can be purified on the basis of their ability to form unstable aggregates during aeration. These aggregates can be solubilized in 60% ethanol (Takei and Richards, 1978).

The purification scheme established was based on the ability of the protein to self-assemble, a characteristic common to hydrophobins. Cultures of *M. grisea* were grown under conditions of nitrogen starvation (Talbot et al., 1993a) and labeled with $^{35}SO_4^{2-}$. The culture filtrate was removed and mixed vigorously on a vortex mixer to ensure aggregation of any secreted hydrophobins; this suspension was made 60% with respect to ethanol. This step divides the hydrophobins into the two groups: class I ethanol-insoluble proteins and class II ethanol-soluble proteins. Both samples were subsequently processed (see Methods). The class I hydrophobin fraction was first extracted with hot SDS, and the SDS-insoluble material was collected, washed extensively with water, and then extracted with ice-cold 100% TFA. The class II hydrophobin fraction was processed by trichloroacetic acid (TCA) precipitation, acetone washing, extensive drying, and then TFA extraction.

Fractions processed in this way were derived from a *mpg1::Hph* transformant (TM400-2) and from strain Guy-11, and they were analyzed by SDS-PAGE autoradiography (Figure 5). Four fractions were analyzed in all: total secreted (TCA precipitable) protein (Figure 5A); 60% ethanol-soluble, TFA extractable proteins (the class II hydrophobin fraction; Figure 5B); 60% ethanol-insoluble, SDS-soluble proteins (Figure 5C); and 60% ethanol-insoluble, SDS-insoluble, TFA-extractable proteins (the class I hydrophobin fraction; Figure 5D).

A number of clear differences between the secreted protein profiles of TM400-2 and Guy-11 were observed. The most prominent of these were differences in the relative abundance of a 33.5-kD protein from the class II hydrophobin fraction in Guy-11 as compared with TM400-2, and differences in the relative abundance of a number of low molecular mass proteins ranging in size from 10 to 18 kD. Conversely, a 42.1-kD protein was found to be relatively more abundant in the *mpg1*$^-$ mutant TM400-2. Prolonged autoradiographic exposures showed that these differences were due to relative abundance and not to the presence or absence of proteins (data not shown). In the class I hydrophobin fraction, however, a 15-kD protein was identified in Guy-11. This protein was completely absent from TM400-2 (Figure 5D). The protein was part of a small complex of bands that were the only major proteins found in this fraction of Guy-11, although a number of faint higher molecular mass bands were also observed after silver staining (data not shown). The protein represented 3% of the secreted total TCA-precipitable radioactivity. In TM400-2, no proteins were observed in the class I hydrophobin fraction, even after long autoradiographic exposures.

If the 15-kD protein missing from the *mpg1::Hph* strain is a hydrophobin, its oxidation with performic acid should result in the conversion of cysteine residues to cysteic acid, breaking any disulfide bridges present in the protein. This oxidation results in monomeric hydrophobins with a reduced electrophoretic mobility (Wessels et al., 1991a; de Vries et al., 1993). Figure 6 shows the 15-kD protein undergoing a mobility shift from an apparent molecular mass of 15 kD after TFA extraction (Figure 6A) to 19.5 kD after performic acid oxidation (Figure 6B). This characteristic suggests that the identified 15-kD protein is a hydrophobin and very likely contains intramolecular disulfide bridges.

To determine whether the identified hydrophobin was also present in the fungal cell walls, extractions were performed from submerged grown mycelium. The mycelium was disrupted in an X-press (Biotec, Stockholm, Sweden), and total protein

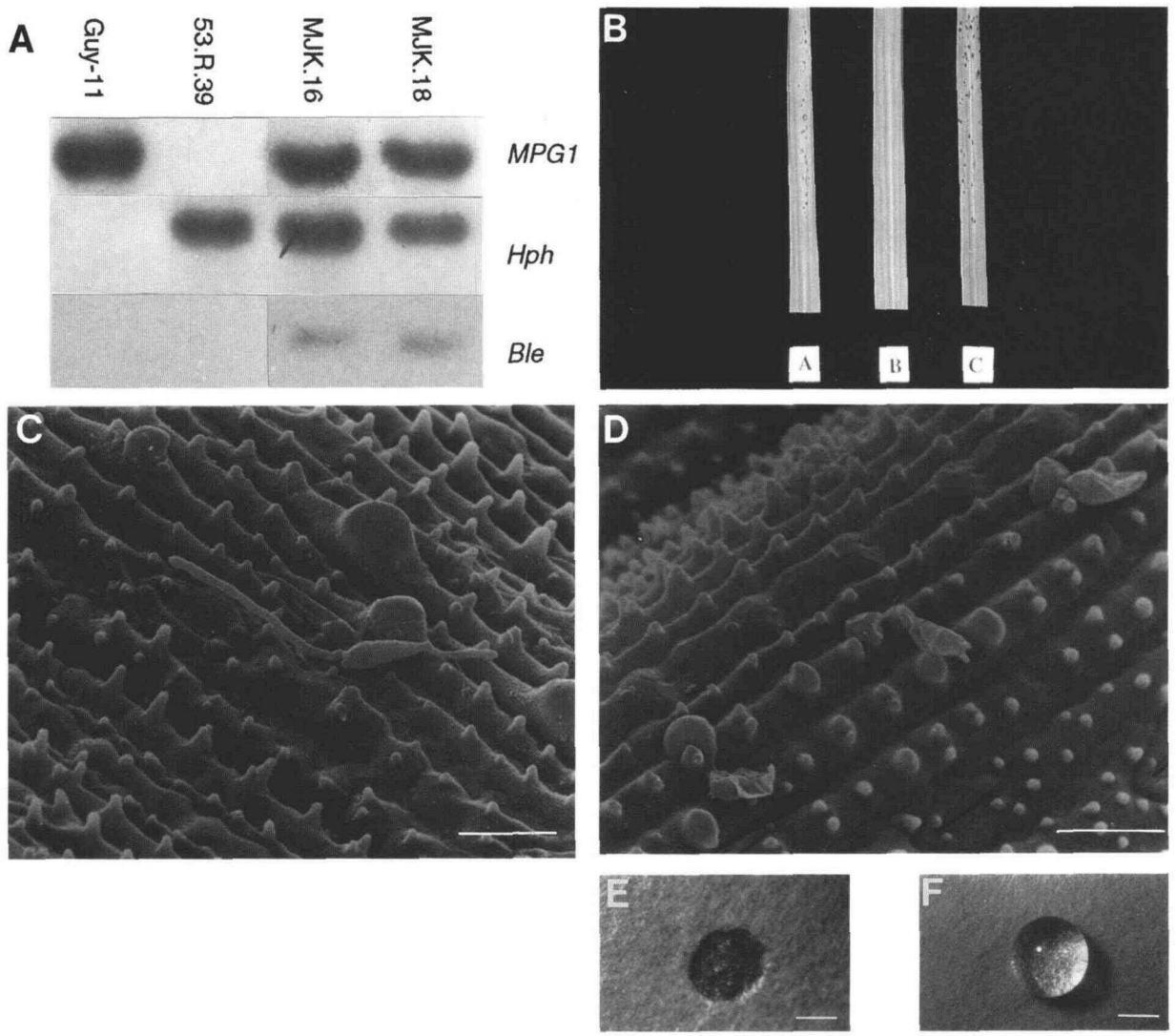

Figure 3. Reintroduction of *MPG1* Restores Pathogenicity, Appressorium Development, and Cell Surface Hydrophobicity.

(A) DNA gel blot analysis of bleomycin-resistant transformants containing the *MPG1* gene. In the top panel, DNA was digested with XbaI and HindIII, fractionated on 0.8% agarose gels, blotted, and hybridized with a 3.75-kb XbaI-HindIII fragment from pNT800 containing the *MPG1* gene. In the middle panel, DNA was digested with XbaI, fractionated on 0.8% agarose gels, blotted, and hybridized with a 2.6-kb XbaI fragment from pNT25 containing the *Hph* gene. At the bottom, DNA was digested with NcoI, fractionated on 0.8% agarose gels, blotted, and hybridized with a 1.16-kb NcoI-XbaI fragment from pAN8-1 containing the bleomycin resistance gene (*Ble*) and *trpC* terminator. This probe hybridized with a 1.7-kb NcoI fragment in bleomycin-resistant transformants. Transformants MJK16 and MJK18 were selected and analyzed for complementation of the Mpg1 phenotypes.

(B) Conidial suspensions prepared from *MPG1* transformants and sprayed onto 14-day-old seedlings of the compatible rice cultivar CO-39. The plants were incubated to allow disease development for 96 hr. Leaves shown are from plants inoculated with the following strains: leaf A, Guy-11; leaf B, 53-R-39; and leaf C, MJK16. Two independent *MPG1* transformants showed the same result in three duplications of the experiment.

(C) and **(D)** Appressorium development on rice leaves assessed in *MPG1* transformants. Scanning electron microscopy of the surface of rice leaves inoculated with *mpg1::Hph* segregant 53-R-39 **(C)** and *MPG1* transformant MJK16 **(D)**. Bars = 20 μm.

(E) and **(F)** Surface hydrophobicity of sporulating cultures assessed by placing a 10-μL drop of water on the surface of a plate culture for 12 hr. **(E)** shows *mpg1::Hph* segregant 53-R-39, and **(F)** shows *MPG1* transformant MJK16. Bars = 1 mm.

was precipitated with TCA. Following SDS extraction, the insoluble fraction was treated with ice-cold TFA, and the resulting (class I hydrophobin) fraction was analyzed by SDS-PAGE and subsequent autoradiography (Figure 7A). Wild-type and *mpg1*$^-$ strains gave very similar protein profiles, with the exception of the 15-kD protein, which was present as a minor component in Guy-11 mycelium but completely absent from TM400-2. The only other observed difference was a 22.6-kD protein that showed a higher relative abundance in the *mpg1*$^-$ mutant TM400-2 than in Guy-11. The relative paucity of the 15-kD hydrophobin in submerged-grown mycelium suggested that most of the protein is secreted during starvation conditions in monomeric form but self-assembles during aerial or interfacial developmental stages such as conidiation and appressorium formation. To test this hypothesis, we performed SDS-PAGE analysis on filtrates of vigorously aerated cultures that had been grown under conditions of nitrogen limitation. A prominent high molecular mass complex was observed in filtrates of Guy-11. This complex was unable to enter the resolving gel, as shown in Figure 7B, and was completely absent from filtrates of the *mpg1*$^-$ mutant TM400-2.

Hydrophobin extractions were next performed with conidia harvested from aerial hyphae of Guy-11 and TM400-2. Extractions were performed by dry harvesting conidia and selecting the TFA-extractable protein fraction. SDS-PAGE showed a single 15-kD protein from conidia of Guy-11. This protein was completely absent from TM400-2 (Figures 8A and 8B). The conidial protein underwent a mobility shift identical to that of the culture filtrate hydrophobin after extraction with performic acid, resulting in an ~19.5-kD protein (data not shown). The 15-kD protein was detected by silver staining and cosegregated with the presence of the *MPG1* gene in the 53-R progeny. A representative sample is shown in Figure 8. 53-R-8 (Figure 8C) contained the 15-kD protein, which was absent from conidial extracts of the *mpg1*$^-$ segregant 53-R-10 (Figure 8D). The gel shows protein samples extracted from equal numbers of conidia. The *mpg1*$^-$ mutants showed a lower overall amount of extractable protein, but overloading of samples did not reveal the presence of the 15-kD hydrophobin (data not shown). The 15-kD hydrophobin identified in extracted culture filtrates also cosegregated with the *MPG1* gene (data not shown). This pattern suggests that the conidial protein and the secreted culture filtrate protein are the same. Finally, analysis of transformant MJK16 showed that it produced the 15-kD hydrophobin (Figure 8E). From these experiments, we conclude that *MPG1* directs the synthesis of the 15-kD protein. We have provisionally designated this protein MPG1p.

MPG1p Is Involved in Surface Interactions during Infection-Related Morphogenesis

We proposed previously that the *MPG1* gene product could function in attachment at the fungal–plant interface (Talbot et al., 1993a; Wessels, 1994; Talbot, 1995). However, a series of flow chamber experiments using water flow rates of up to 7.5 L min^{-1} failed to remove appressoria or attached germ tubes from either wild-type or *mpg1*$^-$ strains (data not shown). These findings suggested either that MPG1p plays no part in the attachment of germ tubes and appressoria or that attachment is due to multiple extracellular components. To distinguish between these possibilities, 12-hr-old germlings (containing germ tubes and appressoria) on Teflon membranes were subjected to four different treatments: washing with water, incubation in 60% ethanol, boiling in 2% SDS, or sequential exposure to all three treatments. Incubation in 60% ethanol should disrupt carbohydrate-mediated and many protein-mediated attachment processes, but the insolubility of aggregated hydrophobins would prevent their release from surfaces. Similarly, boiling in SDS would eliminate protein-mediated attachment but should not affect a hydrophobin-associated process due to insolubility of hydrophobins in SDS. As a control, TFA extraction was performed because it would be likely to affect all mechanisms of attachment involving short-range hydrophobic interactions. The results from these experiments are given in Figure 9.

Initial incubation in 60% ethanol for 20 min resulted in only a minor reduction in the percentage of germinated conidia remaining attached. However, subsequent boiling in SDS resulted in loss of 73% of the conidia and germ tube combinations from the *mpg1*::*Hph* strains, whereas strain Guy-11 showed only 33% detachment. This difference cosegregated with the *MPG1* gene in the 53-R progeny (Figure 9A). The *mpg1*$^-$ progeny 53-R-10 and 53-R-39 showed significant reduction in germ tube–appressorium attachment after SDS extraction, whereas in wild-type progeny the majority of conidium, germ tube, and appressorium combinations remained attached ($\chi^2 = 69.9$; $P < 0.001$). *MPG1* transformants were also completely restored in their ability to attach to Teflon after extraction with hot SDS (data not shown).

Differences in attachment between *mpg1*$^-$ and wild-type strains could reflect a difference in the frequency of appressorium formation. This hypothesis was tested in two ways. First, the attachment of germ tubes was compared during earlier germination time points when both strains would have a predominance of germ tubes. We observed that germ tubes of both wild-type and *mpg1*::*Hph* strains were unable to attach strongly to surfaces until 8 hr after germination, at which point *MPG1*-mediated (SDS-insoluble) attachment was detected in the wild-type individuals (Figure 9B). The *MPG1*-mediated attachment became more pronounced after 8 hr, and the greatest difference between wild-type and *mpg1*$^-$ strains was observed at the 12-hr time point (Figure 9A). Second, we found that appressorium formation in *mpg1*$^-$ strains was restored by cAMP. Remediation occurred with a mean of 86.6% appressorium formation in *mpg1*$^-$ strains. However, appressoria of *mpg1*$^-$ strains could still be more easily removed by SDS extraction than those of the isogenic wild type, as shown in Figure 9C. TFA extraction resulted in almost complete detachment of germ tubes and appressoria in both wild-type and *mpg1*$^-$

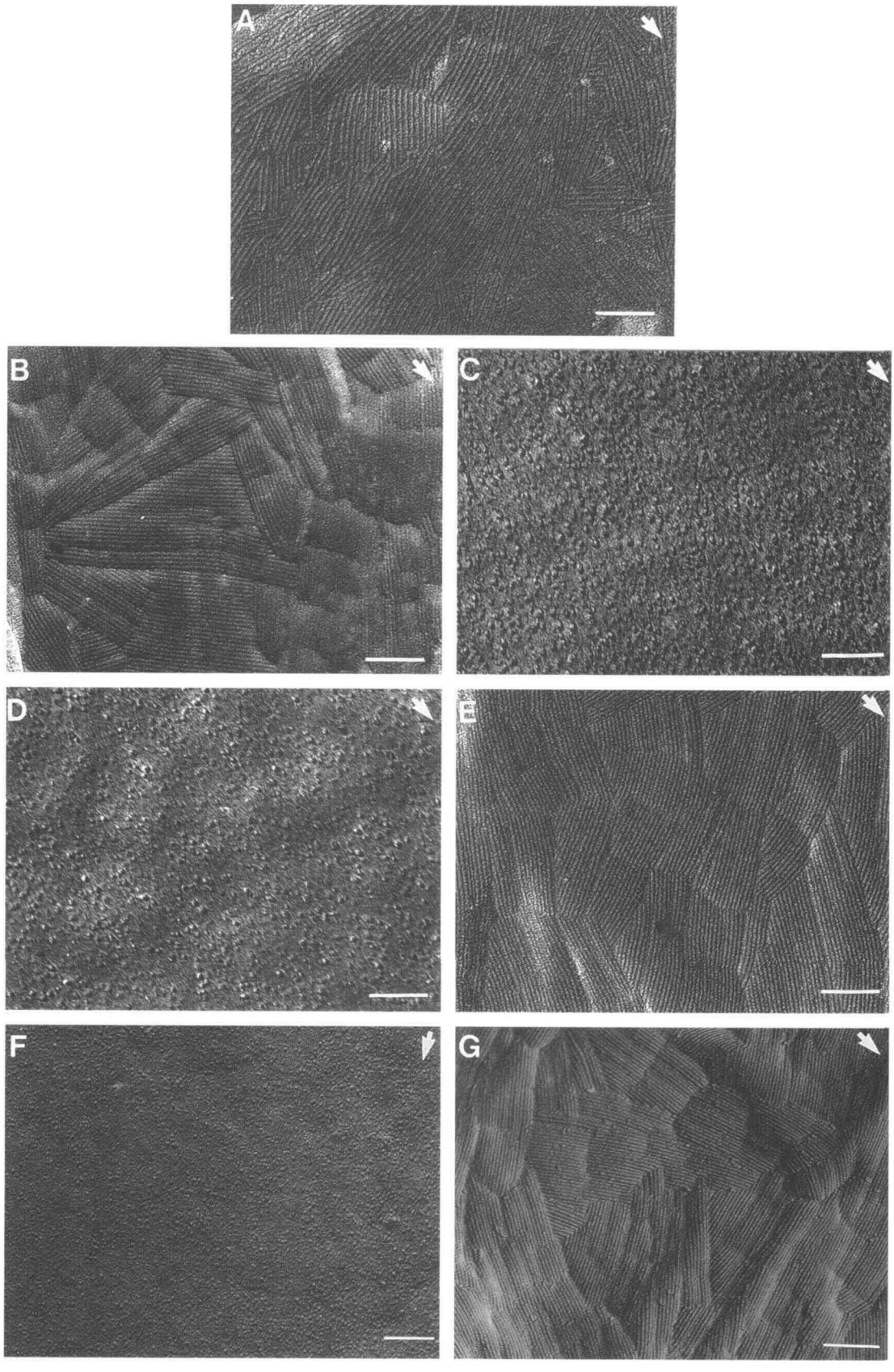

Figure 4. *MPG1* Directs Formation of the Hydrophobic Rodlet Layer of Conidia.

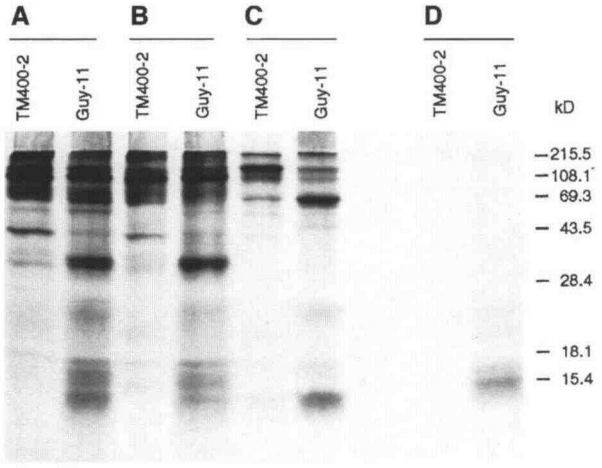

Figure 5. Identification of a 15-kD Hydrophobin from Culture Filtrates of *M. grisea*.

SDS-PAGE autoradiography of ^{35}S-labeled proteins from culture filtrates of *M. grisea* grown under conditions of nitrogen starvation is shown. **(A)** to **(D)** show protein fractions from a scheme designed to identify the product of *MPG1* and determine whether it is a class I or class II hydrophobin. Extractions were performed from cultures of the wild-type strain Guy-11 and the *mpg1*::*Hph* transformant TM400-2. Molecular mass markers are given at right in kilodaltons.
(A) Total TCA-precipitable and TFA-extracted proteins.
(B) Sixty percent ethanol-soluble, TFA-extracted proteins (class II hydrophobin fraction).
(C) Sixty percent ethanol-insoluble, SDS-extractable proteins.
(D) Sixty percent ethanol-insoluble, SDS-insoluble, TFA-extracted proteins (class I hydrophobin fraction).

mutant strains (data not shown). These results indicate that an SDS-insoluble component plays a central role in the interaction of germ tubes with a hydrophobic surface just before and during the development of appressoria. *Mpg1* null mutants are deficient in this component, regardless of whether they can be induced to form appressoria.

DISCUSSION

The *MPG1* gene product acts as a pathogenicity factor in the rice blast fungus by virtue of a role in the prepenetration phase of development and another role much later in the pathogenic cycle during expression of disease symptoms and conidiation (Talbot et al., 1993a). This study sought to characterize *mpg1*$^-$ mutant phenotypes in detail, assess the physical characteristics of the *MPG1* gene product, and examine the likely consequences of these for their role(s) in the prepenetration phase of pathogenicity.

The *mpg1*$^-$ mutants show a number of distinct phenotypes. Therefore, we performed genetic analysis to determine unequivocally whether all mutant phenotypes are associated with the gene disruption event and thus the defect in pathogenicity.

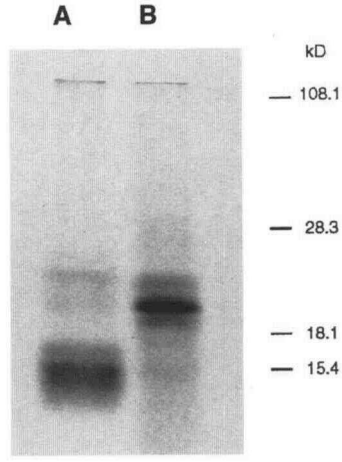

Figure 6. Oxidation of the 15-kD Hydrophobin with Performic Acid.

SDS-PAGE autoradiography of ^{35}S-labeled proteins from a culture of the wild-type strain *M. grisea* Guy-11 is shown. Protein profiles from fraction D of the *MPG1* gene product purification scheme show the electrophoretic mobility of the class I hydrophobin, as follows:
(A) After TFA extraction.
(B) After oxidation with performic acid.
Molecular mass markers are given at right in kilodaltons.

Figure 4. (continued).

Transmission electron microscopy of freeze-fractured conidium surfaces from the following fungal strains:
(A) *A. nidulans* RMS011.
(B) Wild-type *M. grisea* strain Guy-11.
(C) *mpg1*::*Hph* transformant TM400-2.
(D) Hygromycin B–resistant segregant 53-R-10.
(E) Hygromycin B–sensitive segregant 53-R-8.
(F) Hygromycin B–resistant segregant 53-R-39.
(G) A bleomycin-resistant *MPG1* transformant of 53-R-39, MJK16.
The arrows at top right in **(A)** to **(G)** indicate the direction of shadowing. Bars = 100 nm.

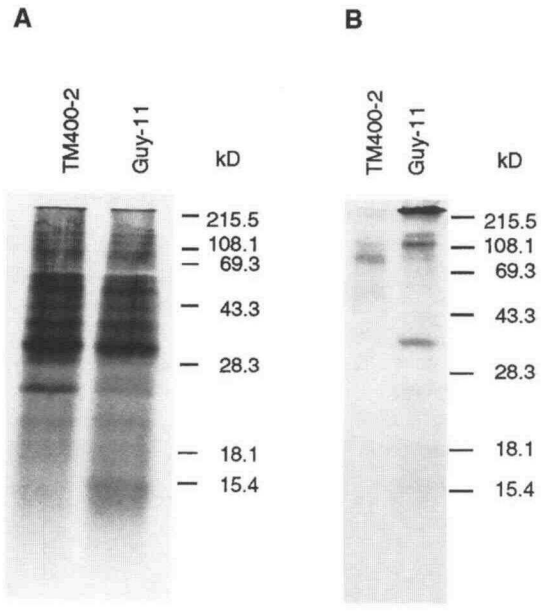

Figure 7. The 15-kD Hydrophobin Is a Component of *M. grisea* Mycelium and Forms High Molecular Weight Complexes after Aeration.

(A) SDS-PAGE autoradiography of ^{35}S-labeled proteins extracted from mycelium of *M. grisea* of the wild-type strain Guy-11 and the *mpg1*::*Hph* transformant TM400-2.

(B) SDS-PAGE autoradiography of ^{35}S-labeled proteins taken directly from the filtrates of vigorously aerated cultures of *M. grisea* that had been grown under conditions of nitrogen starvation. Protein profiles from the wild-type strain Guy-11 and the *mpg1*::*Hph* transformant TM400-2 are shown.

Molecular mass markers are given in kilodaltons at the right of each panel.

This analysis showed that the loss of surface hydrophobicity, reduced conidiation, and reduced appressorium development are all consequences of deletion of the *MPG1* gene, and all of these phenotypes were restored upon reintroduction of the gene. Importantly, appressorium development was also found to be affected directly during development on rice leaf surfaces as well as on inductive inert surfaces. This finding provides the best evidence that loss of pathogenicity in *mpg1*::*Hph* strains is due to the defect in appressorium development. The Mpg1 phenotype appeared more pronounced on rice leaves, and very often germ tubes were found to stop growing just after encountering the waxy projections that cover the rice surface (Figure 2).

Although the DNA sequence of the *MPG1* gene suggested that it encoded a hydrophobin-like protein, it was not clear whether this protein would share the physical characteristics of Sc3p from *S. commune* or would be comparable to ceratoulmin, which is clearly related to fungal hydrophobins (Stringer and Timberlake, 1993). The properties of the 15-kD protein identified in this study most strongly resemble Sc3p, as indicated by the relative shift in the protein's electrophoretic mobility after oxidation by performic acid. Segregation analysis and gene complementation experiments suggest that the synthesis of the 15-kD protein is directed by *MPG1*. Despite high levels of *MPG1* mRNA (Talbot et al., 1993), only small amounts of the 15-kD protein could be detected. Therefore, if *MPG1* encodes this protein, either there are significant post-transcriptional regulation mechanisms, or extraction procedures must be improved before sufficient quantities can be obtained for amino acid analysis.

The putative *MPG1* hydrophobin has an estimated molecular mass of 15 kD compared with a predicted molecular weight of 9.32 kD, based on its predicted amino acid sequence and a presumed signal sequence cleavage site at codon 23 (Heijne, 1983). This discrepancy may be due to glycosylation of the protein, although no consensus N-linked glycosylation sites are apparent in the amino acid sequence of the protein. However, it does contain 12.4% serine and 3.4% threonine residues, which may act as substrates for O-linked glycosylation. Anomalous molecular masses have also been reported for the hydrophobins encoded by *Sc3* and *Sc4* (Schuren and Wessels, 1990; Wessels et al., 1991a) and for cryparin (Zhang et al., 1992); these observations suggest either that hydrophobin proteins interact with carbohydrate or lipid moieties in a number of ways or that their hydrophobicity leads to aberrant electrophoretic mobility.

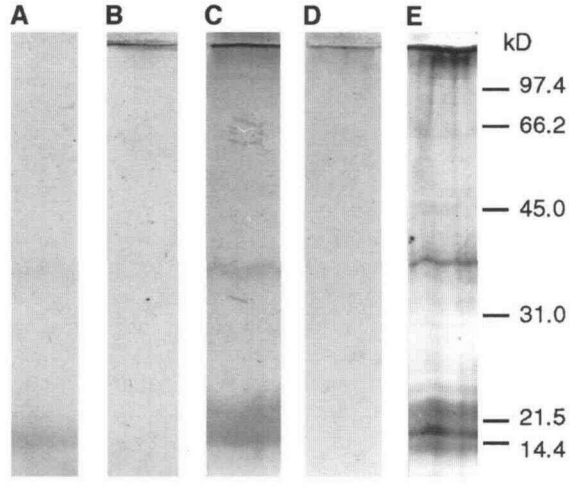

Figure 8. *MPG1* Directs the Production of the 15-kD Hydrophobin.

TFA-extractable proteins were purified from conidia of *M. grisea*. SDS-PAGE was performed using these samples, and the gels were silver stained. Protein profiles are shown from the same number of conidia processed from the following strains:

(A) Guy-11.

(B) *mpg1*::*Hph* transformant TM400-2.

(C) Wild-type segregant 53-R-8.

(D) *mpg1*::*Hph* segregant 53-R-10.

(E) Bleomycin-resistant *MPG1* transformant MJK16.

Molecular mass markers are indicated at right in kilodaltons.

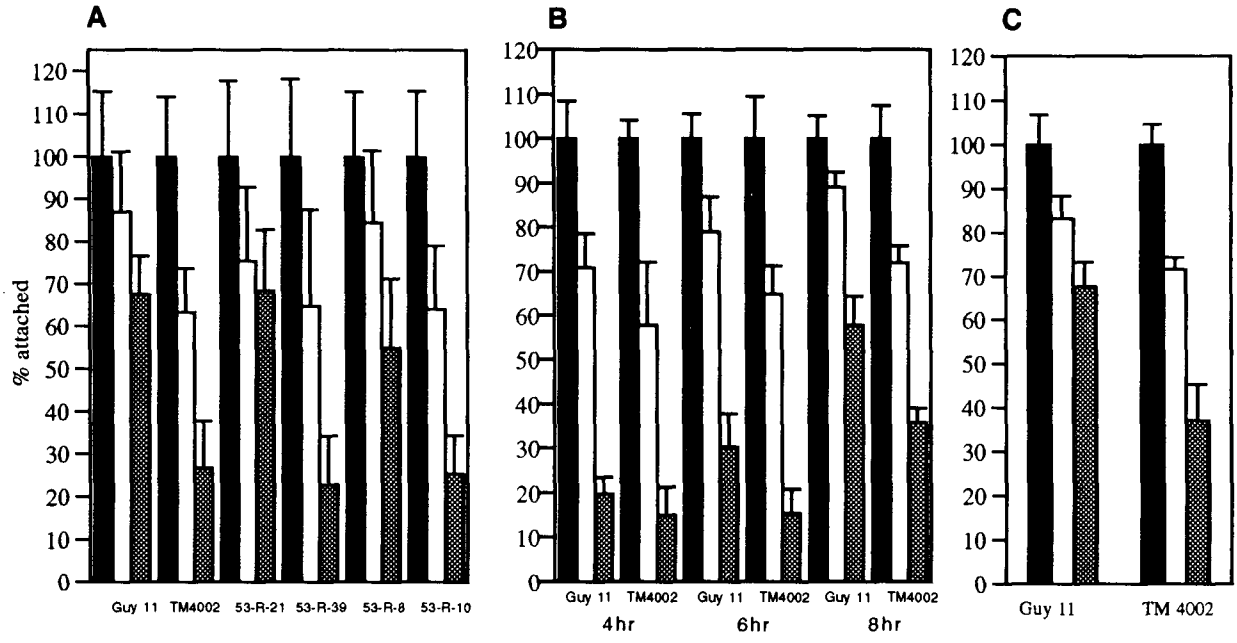

Figure 9. MPG1p Plays a Role in Hydrophobic Surface Interactions of *M. grisea* Germ Tubes and Appressoria.

(A) Bar charts showing the percentage of germinated conidia remaining attached to Teflon surfaces after sequential treatments to detect hydrophobin-mediated processes. Conidia were germinated on Teflon membranes and incubated for 12 hr. At this point, conidia from wild-type strains had elaborated appressoria (mean frequency of appressorium development, 83%), whereas most of those from *mpg1*⁻ mutants had formed long germ tubes (mean frequency of appressorium development, 24.5%). Attached structures were counted after (1) no treatment (black bars); (2) washing in 60% ethanol (white bars); or (3) washing in 60% ethanol followed by boiling for 20 min in 2% SDS (shaded bars). Results are given for the *mpg1*::*Hph* transformant TM400-2, the wild-type Guy-11, *mpg1*::*Hph* progeny 53-R-10 and 53-R-39, and the wild-type progeny 53-R-8 and 53-R-21.
(B) Bar charts showing the percentage of germ tubes remaining attached to Teflon surfaces at three time points after conidium germination. Germination rates were close to 100% in all experiments for both the wild type and *mpg1*⁻ mutants. Treatments were as described above. At 4 hr, short germ tubes had formed in both strains. At 6 hr, appressoria had not formed fully in either Guy-11 or TM400-2, although terminal germ tube swellings were apparent in both. At 8 hr, Guy-11 had formed appressoria (mean, 83.1%), whereas TM400-2 had not (mean, 24%).
(C) Bar chart showing the results of attachment assays after remediation of the Mpg1 appressorium deficiency phenotype with 10 mM of cAMP. Conidia were allowed to germinate for 24 hr until appressoria had elaborated fully (means for Guy-11 and TM400-2 were 85 and 86.6%, respectively). At this point, they were treated as described above. Significantly fewer appressoria of the *mpg1*::*Hph* transformant TM400-2, as compared with those of the wild-type Guy-11, were able to adhere to Teflon after treatment with hot SDS.
Error bars indicate the standard deviation.

The *mpg1*⁻ mutants showed a number of differences in the relative abundance of other secreted proteins in addition to the presence or absence of the putative MPG1p. These differences in abundance may represent pleiotropic effects of the *mpg1*⁻ mutation on the production, secretion, or extraction of other proteins. This possibility was suggested by the fact that many of these differences clearly cosegregated with the presence of *MPG1* (data not shown). Investigation of these differences might therefore shed light on the interactions that hydrophobins may have with other cell wall or extracellular protein components.

The putative *MPG1* hydrophobin appears to self-assemble at an air–water interface. This was suggested by the presence of an insoluble high molecular mass complex in culture filtrates of wild-type *M. grisea* strains after aeration. These complexes were not formed by *mpg1*⁻ mutants. Furthermore, a hydrophobic rodlet layer on the surface of conidia was completely absent from *mpg1*⁻ mutants. The presence of this spore wall layer cosegregated with *MPG1* and was restored upon reintroduction of the gene. We conclude that *MPG1* directs the synthesis of the conidial rodlet layer of *M. grisea*.

Intriguingly, the rodlets were very small, having an estimated diameter of only 5 to 7 nm, compared with the larger rodlets observed on conidia of *A. nidulans* (~10 to 13 nm), *N. crassa* (~11 to 13 nm), and *S. commune* (~13 nm). The significance of this size difference is unknown, although the observation raises the possibility that rodlet size is an indicator of the physical characteristics of a constituent hydrophobin. These proteins are, for example, clearly diverse in both amino acid sequence and net hydropathy (Wessels, 1994). The distribution of hydrophobic residues in MPG1p appears distinct from the products of the *Sc3*, *Sc1*, *Sc4*, *rodA* (*rodletless*), and *EAS/ccg-2*

(*easily-wettable/clock-control gene*) genes, as recently noted by Stringer and Timberlake (1995). They identified a second hydrophobin from *A. nidulans*, called *dewA* (*detergent wettable*), which strongly resembles *MPG1* in the distribution of hydrophobic residues throughout its amino acid sequences, and proposed that *MPG1* and *dewA* form a separate subclass of hydrophobins distinct from the other class I proteins (Stringer and Timberlake, 1995). The dewA protein localizes to the surface of conidia, based on epitope tagging experiments, suggesting that it forms part of the spore rodlet layer with the *rodA* hydrophobin (Stringer and Timberlake, 1995). However, freeze–fracture observations of *dewA*$^-$ mutants show the presence of rodlets that are indistinguishable from those on conidia of wild-type *A. nidulans*, such as those shown in Figure 4A (M.J. Kershaw and N.J. Talbot, unpublished data). The fact that *MPG1* directs formation of a rodlet protein, whereas *dewA* apparently does not, highlights the diversity of function shown by hydrophobins.

Role of *MPG1* in Infection-Related Development

The most striking feature of the *mpg1*$^-$ mutation is the loss of appressorium formation and a reduced ability to elaborate conidia from aerial hyphae. Thus, loss of *MPG1* results in disruption of two distinct developmental pathways. This pattern contrasts with that shown by the mutation of spore rodlet proteins in *A. nidulans* and *N. crassa*. Mutation of the genes encoding these proteins results in a reduction of surface hydrophobicity but not conidial number (Stringer et al., 1991; Bell-Pederson et al., 1992; Stringer and Timberlake, 1995). This finding suggests that conidiation and appressorium formation in *M. grisea* involve related MPG1p-mediated processes.

Conidiation in *M. grisea* involves the production of whorls of conidia found at the end of undifferentiated aerial hyphae (Ou, 1985). These whorls are produced from the center of rice blast lesions under humid conditions, with conidia being distributed by water droplets to adjacent plants. Meanwhile, appressoria form at the hydrophobic interface with the rice leaf after spore germination and germ tube extension (Bourett and Howard, 1990). Therefore, the processes clearly involve water–air or water–hydrophobic surface interactions, which would induce self-assembly of a secreted hydrophobin. Self-assembly of MPG1p on the rice surface before or during appressorium development would provide an effective mechanism for adherence to such a hydrophobic surface. The results of our attachment assays suggest that the adhesion of germ tubes and appressoria has multiple components. This finding is consistent with reports that both carbohydrate- and protein-mediated processes are required for appressorial adhesion (Xiao et al., 1994).

Sequential detachment treatment, modeled on the MPG1p purification scheme, suggests that hydrophobin-mediated events may form part of the attachment process of both germ tubes and appressoria. However, the tight adhesion shown by *mpg1*$^-$ mutants suggests additional roles in infection-related development. One possibility is that the presence of the hydrophobin, perhaps with a localized distribution, is important in achieving the correct cell wall conformation for subsequent development. In this way, the hydrophobin might act as a sensor for the hydrophobic leaf surface. The physical characteristics of the protein, particularly its ability to polymerize at a hydrophobic interface, would allow it to prime the leaf surface for subsequent development of the appressorium. Increasing the wettability of the cuticle would also allow hydrophilic mucilages to act efficiently in appressorium adhesion. The reduced frequency of appressorium development in *mpg1*::*Hph* strains suggests that the surface interaction of the MPG1 protein may serve as an inductive cue for appressorium morphogenesis. This finding is supported by the observation that the *mpg1*$^-$ appressorium-deficient phenotype is remediated by cAMP (J.L. Beckerman and D.J. Ebbole, manuscript submitted), indicating that its action is upstream of a signal transduction pathway required for appressorium elaboration (Lee and Dean, 1993; Mitchell and Dean, 1995).

The hydrophobins are likely to be a ubiquitous class of fungal proteins (de Vries et al., 1993; Bidochka et al., 1995; Templeton et al., 1995). Previous evidence has suggested that their primary role is in aerial morphogenesis (Chasan, 1991; Wessels et al., 1991b) or in surface adhesion (Wösten et al., 1994b). However, the developmental consequences of the *mpg1*$^-$ mutation suggested that this hydrophobin could have other functions in fungal morphogenesis and pathogenicity (Talbot et al., 1993a). In this article, we have shown that the ability of MPG1p, an apparent spore wall protein, to self-assemble may have been co-opted by *M. grisea* into serving a role in surface perception, a process central to the development of its infection structures. This result raises the possibility that plant pathogenic fungi have recruited hydrophobins for critical surface interactions. This evolutionary development may have taken two possible routes: either hydrophobins have intrinsic properties that enable them to self-assemble dependent on the prevailing physical properties of a surface, or specific regulatory pathways have evolved to secrete "generic" hydrophobins at critical times during infection-related development. The diversity of cloned fungal hydrophobins and the genetic tractability of *M. grisea* will allow testing of this idea.

METHODS

Fungal Isolates

Strains of *Magnaporthe grisea* used in this study are stored in the laboratory of N.J. Talbot (Exeter University, Exeter, UK). Strain TH3 was very kindly supplied by Dr. J.L. Notteghem (Centre de Coopération Internationale en Recherche Agronomique pour le Développement, Montpellier, France). The fungus was grown on oatmeal agar and complete medium (Talbot et al., 1993a), using standard procedures (Crawford et al., 1986). Long-term storage of *M. grisea* was performed by growing the fungus through sterile filter paper discs, desiccating these for 48 hr, and storing them at −20°C.

Genetic Crosses

Genetic crosses were performed as described by Valent et al. (1991). Briefly, strains of opposite mating type were paired on oatmeal agar and grown until the mycelia joined. Approximately 12 days after inoculation, flask-shaped perithecia were visible at the mycelial margins. These were transferred to a 4% distilled water agar plate with use of fine forceps. The perithecia were rubbed gently to remove adhering mycelium and conidia before being broken open to reveal asci. Mature asci were removed with a glass needle, and ascospores were dissected from them. These ascospores were transferred individually to a 24-well cell well plate containing complete medium and incubated for 4 to 5 days (Talbot et al., 1993a). At this time, monoconidial isolations were made from each well and grown on individual plates for storage.

Rice Infections

Fourteen-day-old rice seedlings were infected with conidial suspensions of *M. grisea* strains prepared in 0.1% gelatin at a concentration of 10^4 conidia mL^{-1}. Seedlings were sprayed using an artist's airbrush (Badger Co., Franklin Park, IL), and plants were incubated in a controlled environmental growth chamber at 24°C with a 12-hr-light and a 12-hr-dark cycle for 96 to 120 hr, until disease symptoms became apparent. Lesions were counted, and mean lesion densities were determined from randomly chosen 5-cm-long leaf tips. Mean lesion densities were compared using Student's *t* test based on 982 independent observations of leaves infected with either wild-type or *mpg1*$^-$ mutant strains (degrees of freedom, 980).

Assays for Infection-Related Morphogenesis

Appressorium development by *M. grisea* was observed on Teflon membranes (Du Pont), as described by Hamer et al. (1988). A 200-μL drop of a conidial suspension at a concentration of 10^3 mL^{-1} was placed on the surface of a Teflon coverslip and left in a humid environment at 24°C. The frequency of appressorial formation was determined by counting the number of appressoria that had developed from 300 conidia after 14 hr (Talbot et al., 1993b). Appressorium development on rice leaves was examined by incubating suspensions of conidia on rice leaves in a humid chamber for 18 hr at 24°C. Rice leaves were then excised, fixed in 3% glutaraldehyde, treated with 1% osmic acid, and dehydrated in a series of acetone washes. Leaves were then critical-point dried, mounted on stubs, and sputter-coated with palladium gold before viewing with a scanning electron microscope (model S100; Cambridge Instruments, Cambridge, UK).

DNA Isolation and Analysis

Genomic DNA was extracted from fungal mycelium by using a CTAB (hexadecyltrimethyl-ammonium bromide) procedure described by Talbot et al. (1993b). Gel electrophoresis, restriction enzyme digestion, and DNA gel blot hybridizations were all performed using standard procedures (Sambrook et al., 1989). DNA hybridization probes were labeled by the random primer method (Feinberg and Vogelstein, 1983), using the Prime-It kit (Stratagene), and high-stringency washes were performed as described previously by Talbot et al. (1993a).

Complementation of *mpg1::HpH*

The complementation vector pNT800 was constructed by first subcloning a 3.75-kb XbaI-HindIII fragment from λ15g-1 (Talbot et al., 1993a) containing a full-length copy of *MPG1* into pBCKS+ (Stratagene) to create pNT600. The bleomycin resistance gene was excised as a 1.96-kb SacI-XbaI fragment from pAN8-1 (Punt et al., 1987) and subcloned into pNT600 to create the transformation vector pNT800. Fungal transformations were performed as described previously by Talbot et al. (1993a), and bleomycin-resistant transformants were selected at 35 μg mL^{-1} bleomycin (Cayla, Toulouse, France) in the presence of 100 μg mL^{-1} caffeine (Sigma).

Hydrophobin Purification from Culture Filtrates

Liquid cultures of isogenic *M. grisea* strains Guy-11 (wild type) and TM400-2 (*mpg1::Hph*) were prepared in modified minimal media (10 g L^{-1} glucose, 0.1% [v/v] trace elements, 0.01% thiamine, 0.001% biotin, 6 g L^{-1} $NaNO_3$, 0.5 g L^{-1} KCl, 0.4 g L^{-1} $MgCl_2$, 1.5 g L^{-1} KH_2PO_4, pH 6.5) labeled with 40 μCi mL^{-1} $^{35}SO_4^{2-}$, which was added in the form of Na_2SO_4 (Amersham). Cultures were grown for 7 days at 24°C with gentle shaking (100 rpm) under conditions of nitrogen-limiting growth. The mycelium was removed by filtration, rinsed briefly in sterile minimal medium (MM), and squeezed dry before being snap-frozen in liquid N_2 and stored at −20°C. The filtrate (30 mL) was retained, and 30 μL was removed for scintillation counting. At this point, a second 900-μL fraction was removed for direct visualization by SDS-PAGE. This fraction was mixed immediately in 300 μL of 4 × SDS sample buffer and stored at 4°C. A third 900-μL fraction was removed for total protein analysis by trichloroacetic acid (TCA) precipitation. Ice-cold TCA was added to 10% final volume, and proteins were precipitated on ice for 2 hr. The mixture was centrifuged at 5000 rpm and washed twice in 10% TCA, 10 mM $MgSO_4$. The pellet was finally washed twice in ice-cold acetone and dried. The material was resuspended in ice-cold 100% trifluoroacetic acid (TFA). The suspension was centrifuged, and the supernatant was taken to dryness in a gentle stream of nitrogen gas. The dried material was then resuspended in SDS sample buffer for subsequent electrophoresis.

The remaining 30 mL of filtrate was then mixed vigorously with air for 2 min at 44,000 rpm, using a high-speed blender (Sanyo, Tokyo, Japan). Ethanol was added to 60% final volume, and the filtrate was allowed to stand at room temperature for 20 min. The filtrate was centrifuged at 3440*g* for 1 hr, and the supernatant and pellet were both retained.

The 60% ethanol-soluble fraction was processed by first evaporating away the ethanol in a rotovac. TCA was then added to 10% final volume, and the solution was incubated for 2 hr on ice. The solution was then centrifuged at 3440*g* for 30 min, and the precipitated proteins were retained. The pellet was washed twice in 10% TCA, with a final wash in acetone. At this point, the pellet was dried on the bench for 15 min and resuspended in ice-cold 100% TFA. The suspension was centrifuged, and the supernatant was taken to dryness in a gentle stream of nitrogen gas. The dried material was then resuspended in SDS sample buffer.

The 60% ethanol-insoluble fraction was processed by first washing twice in 60% ethanol and then centrifuging at 3440*g* for 30 min each time. The pellet was extracted in 1% SDS at 100°C for 20 min. The suspension was centrifuged at 3440*g*, and the supernatant and pellet were both retained. The SDS-soluble protein fraction was stored for analysis by electrophoresis. The SDS-insoluble fraction was further processed by washing twice with 1% SDS containing 10 mM $MgSO_4$

and twice with sterile distilled water. The pelleted material was then lyophilized before being resuspended in ice-cold 100% TFA. The mixture was sonicated briefly on ice, and the suspension was centrifuged at 4°C. The supernatant was then taken to dryness in a gentle stream of nitrogen gas. The dried material was finally resuspended in SDS sample buffer.

Hydrophobin Purification from Fungal Mycelium and Conidial Walls

Mycelium from $^{35}SO_4^{2-}$ labeling experiments was processed using an X-press (Biotec), and protein precipitations were performed with TCA. The total TCA-precipitated material was extracted by boiling in 1% SDS for 20 min. SDS-insoluble material was retained and washed extensively in double-distilled H_2O. After lyophilization, the pellet was extracted with ice-cold 100% TFA, dried in a stream of N_2 gas, and resuspended in SDS sample buffer.

Conidia were harvested from cultures of *M. grisea* by gentle washing with ice-cold 100% TFA. The suspension was dried gently in a stream of nitrogen gas and vacuum desiccated overnight in the presence of solid NaOH. The dried material was resuspended in SDS sample buffer, centrifuged to remove conidial debris, and stored at 4°C.

Analytical Procedures

SDS-PAGE of radioactive proteins was performed using standard procedures (Laemmli, 1970). Gels were routinely 12.5 or 15% (w/v) polyacrylamide. Samples taken up in SDS sample buffer after TFA treatment were adjusted to pH 6.8 with 1 M Tris. Autoradiography was performed directly on gels that had been dried at 65°C, using Kodak X-OMAT or Amersham Hyperfilm. Where appropriate, fluorography was performed by soaking gels in 1 M sodium salicylate, drying them, and exposing them to x-ray film at −70°C (Chamberlain, 1979). Silver staining was performed using a commercial kit, according to the manufacturer's instructions (Bio-Rad).

Electron Microscopy

Rodlet layers were viewed as replicas made at room temperature or after freeze etching. Conidia were vacuum evaporated in an evaporator (model 301; Baltzer Pfeiffer GmbH, Baltzer, Liechtenstein) and shadowed with carbon and platinum at 45°C. A backing layer of pure carbon was added at 90°C, and the replicas were floated onto distilled water. Replicas were cleaned overnight in 50% chromic acid and washed several times in distilled water before being picked up onto copper grids and viewed with a microscope (model 100C; Jeol, Tokyo, Japan). For freeze–fracture studies, concentrated conidia were fixed in 3% glutaraldehyde in 100 mM potassium phosphate buffer (pH 7.0) and washed three times in buffer by a modification of the procedure of Stringer et al. (1991). Samples were then cryoprotected by sequential infiltration with 10% (1 hr) and 20% (overnight) glycerol. Samples were placed in Baltzer's specimen holders and frozen in Freon 22 (ICI, Runcorn, UK) and liquid nitrogen. Fracturing was performed in a Baltzer's 301 evaporator and processed as described for room temperature replicas.

Fungal Attachment Assays

Conidia were allowed to germinate for 12 hr on Teflon membranes (Du Pont) at 24°C in the dark. Attachment assays were performed with simple washing experiments under a flowing tap or performed in a flow chamber on a Universal microscope stage (Carl Zeiss, Oberkochen, Germany).

Experiments to investigate hydrophobin-mediated processes were performed by sequential treatment of germinated conidia, germ tube, and appressorial combinations prepared on Teflon membranes. Samples were first treated with 60% ethanol for 20 min at room temperature with gentle shaking. This was followed by boiling in 2% SDS for 20 min in a water bath with gentle inversion of the boiling tube every 2 min. Samples were then rinsed gently in sterile distilled water and examined by microscopy. Several independent experiments were performed to determine the effect of each treatment singly. The percentage of adhering conidia, germ tube, and appressorium combinations from each strain was determined.

Remediation experiments with cAMP were performed by incubation of conidia in 10-mM cAMP (Sigma) solutions, as described by Lee and Dean (1993).

ACKNOWLEDGMENTS

This work was funded by a European Molecular Biology Organization short-term fellowship and a research grant from the Biotechnology and Biological Sciences Research Council to N.J.T. Work on *M. grisea* in the laboratory of N.J.T. is authorized by the Plant Health division of the Ministry of Agriculture, Fisheries and Food license No. PHF 1524/1130/74. J.E.H. is a National Science Foundation Presidential Faculty Fellow.

Received January 31, 1996; accepted April 11, 1996.

REFERENCES

Beever, R.E., and Dempsey, G.P. (1978). Function of rodlets on the surface of fungal spores. Nature **272,** 608–610.

Bell-Pederson, D., Dunlap, J.C., and Loros, J.J. (1992). The *Neurospora* circadian clock–controlled gene, *ccg-2*, is allelic to *eas* and encodes a fungal hydrophobin required for formation of the conidial rodlet layer. Genes Dev. **6,** 2382–2394.

Bidochka, M.J., St. Leger, R.J., Joshi, L., and Roberts, D.W. (1995). The rodlet layer from aerial and submerged conidia of the entomopathogenic fungus *Beauvaria bassiana* contains hydrophobin. Mycol. Res. **99,** 403–406.

Bourett, T.M., and Howard, R.J. (1990). *In vitro* development of penetration structures in the rice blast fungus *Magnaporthe grisea*. Can. J. Bot. **68,** 329–342.

Bowden, C.G., Hintz, W.E., Jeng, R., Hubber, M., and Horgen, P. (1994). Isolation and characterization of the cerato-ulmin toxin gene of the Dutch elm disease pathogen *Ophiostoma ulmi*. Curr. Genet. **25,** 223–229.

Chamberlain, J.P. (1979). Fluorographic detection of radioactivity in polyacrylamide gels with the water-soluble fluor, sodium salicylate. Anal. Biochem. **98,** 132–135.

Chasan, R. (1991). Building hyphae in the air. Plant Cell **3,** 1048–1050.

Crawford, M.S., Chumley, F.G., Weaver, C.G., and Valent, B. (1986). Characterization of the heterokaryotic and vegetative diploid phases of *Magnaporthe grisea*. Genetics **114,** 1111–1129.

de Vries, O.M.H., Fekkes, M.P., Wosten, H.A.B., and Wessels, J.G.H. (1993). Insoluble hydrophobin complexes in the walls of *Schizophyllum commune* and other filamentous fungi. Arch. Microbiol. **159,** 330–335.

Feinberg, A.P., and Vogelstein, B. (1983). A technique for radiolabeling DNA restriction fragments to high specific activity. Anal. Biochem. **132,** 6–13.

Hamer, J.E., Howard, R.J., Chumley, F.G., and Valent, B. (1988). A mechanism for surface attachment of spores of a plant pathogenic fungus. Science **239,** 288–290.

Heijne, G.V. (1983). Patterns of amino acids near signal sequence cleavage sites. Eur. J. Biochem. **133,** 17–21.

Laemmli, U.K. (1970). Cleavage of structural proteins during the assembly of the head of bacteriophage T4. Nature **227,** 680–685.

Lauter, F.R., Russo, V.E.A., and Yanofsky, C. (1992). Developmental and light regulation of *Eas*, the structural gene for the rodlet protein of *Neurospora crassa*. Genes Dev. **6,** 2373–2381.

Lee, Y. H., and Dean, R.A. (1993). cAMP regulates infection structure formation in the plant pathogenic fungus *Magnaporthe grisea*. Plant Cell **5,** 693–700.

Lee, Y.H., and Dean, R.A. (1994). Hydrophobicity of contact surface induces appressorium formation in *Magnaporthe grisea*. FEMS Microbiol. Lett. **115,** 71–75.

Mendgen, K., and Deising, H. (1993). Infection structures of fungal plant pathogens—A cytological and physiological evaluation. New Phytol. **124,** 193–213.

Mitchell, T.K., and Dean, R.A. (1995). The cAMP-dependent protein kinase catalytic subunit is required for appressorium formation and pathogenesis by the rice blast fungus *Magnaporthe grisea*. Plant Cell **7,** 1869–1878.

Ou, S.H. (1985). Rice Diseases. (Kew, UK: Commonwealth Mycological Institute, Commonwealth Agricultural Bureau).

Punt, P.J., Oliver, R.P., Dingemanse, M.A., Pouwels, P.H., and van den Hondel, C.A.M.J.J. (1987). Transformation of *Aspergillus* based on the hygromycin B resistance marker from *Escherichia coli*. Gene **56,** 117–124.

Sambrook, J., Fritsch, E.F., and Maniatis, T. (1989). Molecular Cloning: A Laboratory Manual. (Cold Spring Harbor, NY: Cold Spring Harbor Laboratory).

Schuren, F.H.J., and Wessels, J.G.H. (1990). Two genes specifically expressed in fruiting dikaryons of *Schizophyllum commune*: Homologies with a gene not regulated by mating type genes. Gene **90,** 199–205.

St. Leger, R.J., Staples, R.C., and Roberts, D.W. (1992). Cloning and regulatory analysis of starvation-stress gene, *ssgA*, encoding a hydrophobin-like protein from the entomopathogenic fungus *Metarhizium anisopliae*. Gene **120,** 119–124.

Stringer, M.A., and Timberlake, W.E. (1993). Cerato-ulmin, a toxin involved in Dutch elm disease, is a fungal hydrophobin. Plant Cell **5,** 145–146.

Stringer, M.A., and Timberlake, W.E. (1995). *dewA* encodes a fungal hydrophobin component of the *Aspergillus* spore wall. Mol. Microbiol. **16,** 33–44.

Stringer, M.A., Dean, R.A., Sewell, T.C., and Timberlake, W.E. (1991). *Rodletless*, a new *Aspergillus* developmental mutant induced by directed gene inactivation. Genes Dev. **5,** 1161–1171.

Takai, S., and Richards, W.C. (1978). Cerato-ulmin, a wilting toxin of *Ceratocystis ulmi*: Isolation and some properties of cerato-ulmin from the culture of *C. ulmi*. J. Phytopathol. **91,** 129–146.

Talbot, N.J. (1995). Having a blast: Exploring the pathogenicity of *Magnaporthe grisea*. Trends Microbiol. **3,** 9–16.

Talbot, N.J., Ebbole, D.J., and Hamer, J.E. (1993a). Identification and characterization of *MPG1*, a gene involved in pathogenicity from the rice blast fungus *Magnaporthe grisea*. Plant Cell **5,** 1575–1590.

Talbot, N.J., Salch, Y.P., Ma, M., and Hamer, J.E. (1993b). Karyotype variation within clonal lineages of the rice blast fungus, *Magnaporthe grisea*. Appl. Environ. Microbiol. **59,** 585–593.

Templeton, M.D., Greenwood, D.R., and Beever, R.E. (1995). Solubilization of *Neurospora crassa* rodlet proteins and identification of the predominant protein as the proteolytically processed *eas (ccg-2)* gene product. Exp. Mycol. **19,** 166–169.

Valent, B., Farrall, L., and Chumley, F.G. (1991). *Magnaporthe grisea* genes for pathogenicity and virulence identified through a series of backcrosses. Genetics **127,** 87–101.

Wessels, J.G.H. (1992). Gene expression during fruiting in *Schizophyllum commune*. Mycol. Res. **96,** 609–620.

Wessels, J.G.H. (1994). Developmental regulation of fungal cell wall formation. Annu. Rev. Phytopathol. **32,** 413–437.

Wessels, J.G.H., de Vries, O.M.H., Ásgeirsdóttir, S.A., and Schuren, F.H.J. (1991a). Hydrophobin genes involved in formation of aerial hyphae and fruit bodies in Schizophyllum. Plant Cell **3,** 793–799.

Wessels, J.G.H., de Vries, O.M.H., Ásgeirsdóttir, S.A., and Springer, J. (1991b). The *thn* mutation of *Schizophyllum commune*, which suppresses formation of aerial hyphae, affects expression of the *Sc3* hydrophobin gene. J. Gen. Microbiol. **137,** 2439–2445.

Wösten, H.A.B., de Vries, O.M.H., and Wessels, J.G.H. (1993). Interfacial self-assembly of a fungal hydrophobin into a hydrophobic rodlet layer. Plant Cell **5,** 1567–1574.

Wösten, H.A.B., Ásgeirsdóttir, S.A., Krook, J.H., Drenth, J.H.H., and Wessels, J.G.H. (1994a). The fungal hydrophobin Sc3p self-assembles at the surface of aerial hyphae as a protein membrane constituting the hydrophobic rodlet layer. Eur. J. Cell Biol. **63,** 122–129.

Wösten, H.A.B., Schuren, F.H.J., and Wessels, J.G.H. (1994b). Interfacial self-assembly of a hydrophobin into an amphipathic membrane mediates fungal attachment to hydrophobic surfaces. EMBO J. **13,** 5848–5854.

Wösten, H.A.B., Ruardy, T.G., Van der Mei, H.C., Busscher, H.J., and Wessels, J.G.H. (1995). Interfacial self-assembly of a *Schizophyllum commune* hydrophobin into an insoluble amphipathic membrane depends on surface hydrophobicity. Colloids Surf. B. **5,** 189–195.

Xiao, J.Z., Ohshima, A., Kamakura, T., Ishiyama, T., and Yamaguchi, I. (1994). Extracellular glycoprotein(s) associated with cellular differentiation in *Magnaporthe grisea*. Mol. Plant-Microbe Interact. **7,** 639–644.

Zhang, L., Villalon, D., Sin, Y., Kazmierczak, P., and Van Alfen, N.K. (1992). Virus-associated down-regulation of the gene encoding cryparin, an abundant cell surface protein of the chestnut blight fungus *Cryphonectria parasitica*. Gene **139,** 59–64.